

COUPLED MAGNETOHYDRODYNAMIC OSCILLATIONS
IN THE MAGNETOSPHERE-IONOSPHERE SYSTEM
—HALL CURRENT EFFECT—

Shigeru FUJITA

Meteorological College, 4–81, Asahi 7-chome, Kashiwa 277

Abstract: As the first step to a quantitative study of the magnetohydrodynamic coupled oscillations for the magnetosphere-ionosphere system, we revise the basic equations into a suitable form for computer calculations by means of the finite element method. Numerical analysis is performed by using a simple box model, taking account of the anisotropically conducting ionosphere and the insulating atmosphere. Owing to limited capacity of a computer, the effect of the ionospheric Hall current is discussed. We obtained the following results: (1) The mode conversion effect due to the Hall current gives rise to resonant coupling when the azimuthal wave number is zero (the azimuthal direction is referred to the direction perpendicular to the plane of the box model). (2) The Alfvén mode perturbation is enhanced along the resonant field line but in the case of the fast magnetosonic mode the enhancement does not occur.

1. Introduction

Coupled hydromagnetic (MHD) oscillations are common in the spatially inhomogeneous plasmas. Once the global cavity oscillation with the spatially invariant frequency is generated by impulsive disturbances such as a tangential discontinuity in the solar wind, this oscillation couples with the local field line oscillation (standing Alfvén wave) whose eigen-frequency matches that of the cavity oscillation (KIVELSON and SOUTHWOOD, 1985). The local oscillation is observed as ULF geomagnetic pulsations on the ground.

The coupled MHD oscillations in the magnetosphere has been studied under the assumption of the perfectly conducting ionosphere (*e.g.*, LEE and LYSAK, 1989, 1990, 1991a, b; FUJITA and PATEL, 1992). Some papers considered the dissipation effect of the ionosphere (SOUTHWOOD, 1974; ALLAN *et al.*, 1986a, b; KRAUSS-VARBAN and PATEL, 1988). But when we discuss the theoretical results and the MHD simulations in reference to ground observations of ULF pulsations, it is essential to take account of the anisotropy of the ionospheric conductivity. Furthermore the characteristics of the coupled MHD oscillations in the magnetosphere may depend on the ionospheric condition.

Interaction between the MHD waves and the ionosphere has been studied by a number of researchers (*e.g.*, INOUE and HOROWITZ, 1966a, b; INOUE and SHAEFFER, 1970; INOUE, 1973; HUGHES and SOUTHWOOD, 1976a, b). INOUE (1973) indicated a mode conversion between the Alfvén wave and the fast magnetosonic mode wave (the fast mode wave in the latter part of the present paper) due to the ionospheric Hall

current. Recently the ionospheric interaction of magnetospheric coupled oscillations has been attracted attention of some workers. KIVELSON and SOUTHWOOD (1988) studied qualitatively effects of the ionosphere on magnetospheric coupled MHD oscillations. Their major conclusion is that the ionospheric modification of the coupled oscillations is like the Alfvén wave incidence near a resonant field and like the fast mode wave incidence in a region away from the resonant field. HAMEIRI and KIVELSON (1991) studied analytically ionosphere-atmosphere effects on the coupled oscillations as an extension of KIVELSON and SOUTHWOOD (1988). They theoretically explained the observational fact that the ground pulsations have a larger amplitude in the daytime than in the nighttime. Namely when the ionospheric conductivity is higher (the daytime), the MHD oscillations are almost perfectly reflected so that the previous coupled oscillation theory is valid for this case. Consequently very large amplitude associated with the resonant Alfvén wave is expected in the daytime. On the other hand, in the nighttime when the ionospheric conductivity is low, field-aligned structures of perturbation fields become different between the Alfvén and fast mode waves. Therefore coupled resonance is not effective to enhance the amplitude of the Alfvén wave in the nighttime.

The previous theories on the coupled MHD oscillations in the magnetosphere-ionosphere system are analytical. Therefore it is usually quite difficult to obtain exact solutions even when the magnetosphere is simply modeled. Indeed HAMEIRI and KIVELSON (1991) could show only approximated results. To evaluate realistic values relevant to the coupled oscillations, we will introduce the finite element method (FEM) to calculate the electromagnetic (em) field perturbations of the coupled oscillations in the magnetosphere-ionosphere system. This method has an advantage that it can be used to perform calculations for an arbitrarily shaped model. In the present paper we deal with the formulation of the FEM calculation based on the Galerkin method. Although the FEM calculation can be applied to the realistic magnetospheric model, we use here a simple box model (KIVELSON and SOUTHWOOD, 1985) as a preliminary step to more realistic model calculations.

Only limited results are shown in the present paper. The effect of the ionospheric Hall current is mainly dealt with, because the behavior of the coupled oscillation is clearly reproduced in the preliminary calculation with coarse mesh grids. Resonant oscillations due to the mode coupling associated with the Hall current have not been discussed yet.

We explain the box model and basic equations for the numerical analysis of the coupled MHD oscillations in the magnetosphere-ionosphere system in Section 2. In Section 3 we present numerical results. In Section 4 we give qualitative interpretations on the numerical results.

2. Model and Basic Equations

2.1. Model

The box model which includes the magnetosphere, ionosphere, and atmosphere is employed and is shown schematically in Fig. 1. The ambient magnetic field is along the z axis. The Alfvén speed (V_A) is a function of x and z . Plasmas and the ambient

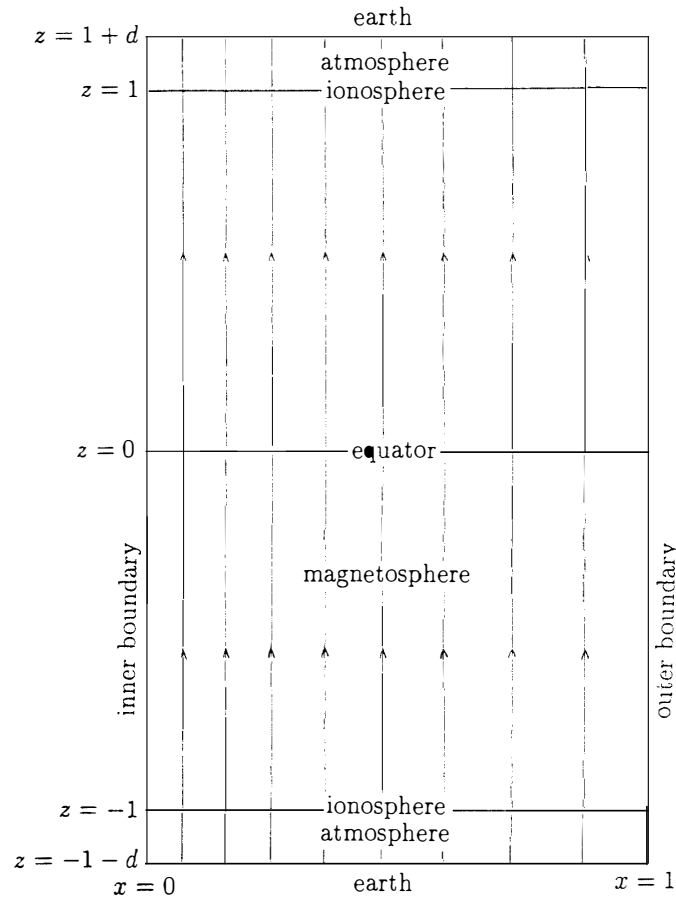


Fig. 1. The box model for the magnetosphere-ionosphere system. The ionosphere is an infinitely thin layer with anisotropic height-integrated conductivities (Σ_P and Σ_H). The insulating atmosphere separates the ionosphere and the perfectly conducting earth.

magnetic field are homogeneous in the y direction. Accordingly the field perturbations of coupled MHD oscillations vary as $\exp(imy - i\omega t)$ where ω is the angular frequency and m is the wave number in the y direction. In the present paper m is zero because we consider the mode conversion due to the ionospheric Hall current. Therefore the condition of $\delta B_y = 0$ (the toroidal magnetic perturbation) in the atmosphere can be used.

This model is divided into 3 regions: the magnetosphere ($|z| < 1$), the infinitely thin ionosphere ($|z| = 1$), and the neutral atmosphere ($1 < |z| < 1 + d$). The perfectly conducting solid earth is located below the atmosphere. The southern and northern hemispheres correspond to regions of negative and positive z , respectively. The boundaries on $x = 0$ and 1 are inner (low latitude) and outer (high latitude) boundaries of the magnetospheric cavity. In the actual magnetosphere, the outer and inner boundaries correspond to the magnetopause and the outer boundary of the plasmapause, respectively (LEE and LYSAK, 1989). The Poynting flux associated with the oscillation is partially reflected at the boundaries. As will be noted later, we assume for simplicity perfect reflection of the Poynting flux both at the x -boundaries. The ambient magnetic field intensity (B_0) and V_A are symmetrical with respect to the equator. Since typical $V_A \ll c$ (the speed of light), c is regarded infinite in our calculations. The ionosphere is

assumed to be a thin layer with the anisotropic height-integrated Pedersen (Σ_P) and Hall (Σ_H) conductivities. The functional form of $V_A(x, z)$ is given as

$$\frac{V_A(x, z)}{V_0} = (\alpha z^2 + 1) \{(\beta - 1)(1 - x) + 1\}. \quad (1)$$

The value V_0 is the Alfvén speed at $(x, z) = (1, 0)$ (the equator of the outer boundary). α and β are free parameters. In the calculations we specify $\alpha = 1$ and $\beta = 4$.

2.2. Boundary Conditions

We must specify the boundary conditions on $x = 0$ and 1 (the inner and outer boundaries) and $|z| = 1 + d$ (the surface of the solid earth). We assume that δE_y (y component of the electric field perturbation) = 0 at $x = 0$ and 1 . This boundary condition means no Poynting flux across the x -boundaries. Electric field perturbations tangential to the ground vanish on $|z| = 1 + d$ because the earth is considered a perfect conductor.

The boundary conditions of the em perturbations just above and just below the ionosphere are as follows:

$$\delta \mathbf{E}_{\perp \text{ mag.}} = \delta \mathbf{E}_{\perp \text{ atm.}}, \quad (2)$$

and

$$-\hat{\mathbf{e}} \times (\delta \mathbf{B}_{\perp \text{ mag.}} - \delta \mathbf{B}_{\perp \text{ atm.}}) = \mu_0 \delta \mathbf{J}_{\text{ionos.}} = \mu_0 (\Sigma_P \delta \mathbf{E}_{\perp \text{ mag.}} + \Sigma_H \hat{\mathbf{e}} \times \delta \mathbf{E}_{\perp \text{ mag.}}), \quad (3)$$

where $\hat{\mathbf{e}} = \mathbf{B}_0 / B_0$. The unit vector $\hat{\mathbf{e}}$ is perpendicular to the ionosphere and is directed outward from the magnetosphere. Thus $\hat{\mathbf{e}} = \hat{\mathbf{e}}$ in the northern hemisphere and $\hat{\mathbf{e}} = -\hat{\mathbf{e}}$ in the southern hemisphere. The electric and magnetic perturbations perpendicular to \mathbf{B}_0 are $\delta \mathbf{E}_{\perp}$ and $\delta \mathbf{B}_{\perp}$. The subscripts “mag.”, “atm.”, and “ionos.” refer respectively to the magnetosphere, atmosphere, and ionosphere. Since \mathbf{B}_0 is perpendicular to the ionosphere in our model, $\delta \mathbf{E}_{\perp}$ is tangential to the ionosphere. The magnetic permeability is denoted by μ_0 .

2.3. FEM Formulation

We show the basic equations for the FEM calculations, including both the ionospheric boundary conditions (eqs. (2) and (3)) and the contribution from the atmosphere. The Galerkin formulation (ZIENKIEWICS and TAYLOR, 1989) is applied to the MHD coupled equations in the magnetosphere. In our case the formulation leads to

$$\begin{aligned} & \int_{\text{mag.}} (\nabla \times \delta \mathbf{E}_{\perp}^*) \cdot (\nabla \times \delta \mathbf{E}_{\perp}) dV - \int_{\text{mag.}} \left(\frac{\omega}{V_A} \right)^2 \delta \mathbf{E}_{\perp}^* \cdot \delta \mathbf{E}_{\perp} dV \\ & - \int_{\text{ionos.}} \{ \delta \mathbf{E}_{\perp}^* \times (\nabla \times \delta \mathbf{E}_{\perp}^u) \} \cdot \hat{\mathbf{e}} dS = 0, \end{aligned} \quad (4)$$

where the superscript u stands for the value just above the ionosphere. When we recall analogy between the variational and Galerkin methods, we notice that the first and second terms in eq. (4) are derived from the potential and the kinetic energy terms, respectively, for the magnetospheric plasma motion (GRUBER and RAPPAZ, 1985). The third term indicates the Poynting flux from the magnetosphere to the ionosphere.

Using eqs. (2) and (3) as well as the relation $\nabla \times \delta \mathbf{E}_\perp^u = i\omega \delta \mathbf{B}$, the third term of eq. (4) can be transformed

$$\begin{aligned} & \int_{\text{ionos.}} \{ \delta \mathbf{E}_\perp^* \times (\nabla \times \delta \mathbf{E}_\perp^u) \} \cdot \hat{\mathbf{e}} dS \\ &= \int_{\text{ionos.}} \{ \delta \mathbf{E}_\perp^* \times (\nabla \times \delta \mathbf{E}^d) \} \cdot \hat{\mathbf{e}} dS + i\omega \mu_0 \Sigma_P \int_{\text{ionos.}} \delta \mathbf{E}_\perp^* \cdot \delta \mathbf{E}_\perp dS \\ & \quad + i\omega \mu_0 \Sigma_H \int_{\text{ionos.}} (\delta \mathbf{E}_\perp^* \times \delta \mathbf{E}_\perp) \cdot (-\hat{\mathbf{e}}) dS, \end{aligned} \quad (5)$$

where the superscript d stands for the value just below the ionosphere. When we consider the corresponding variational form, the second term in r.h.s. of eq. (5) is proportional to the scalar product of $\Sigma_P \delta \mathbf{E}_\perp$ (Pedersen current) and $\delta \mathbf{E}_\perp$. This term physically expresses the ionospheric Joule dissipation. Similarly the third term is the vector product of $\Sigma_H \delta \mathbf{E}_\perp$ (Hall current) and $\delta \mathbf{E}_\perp$. Thus this term leads to no energy dissipation. According to FUJITA and TAMAO (1988) and FUJITA (1988), this term gives rise to the mode conversion between the Alfvén wave and the fast mode wave. The first term expresses the Poynting flux into the atmosphere. This will be connected with em perturbations in the atmosphere. Actually

$$\begin{aligned} & \int_{\text{ionos.}} \{ \delta \mathbf{E}_\perp^* \times (\nabla \times \delta \mathbf{E}^d) \} \cdot \hat{\mathbf{e}} dS \\ &= - \int_{\text{atm.}} (\nabla \times \delta \mathbf{E}_\perp^*) \cdot (\nabla \times \delta \mathbf{E}_\perp) dV - \int_{\text{atm.}} (\nabla \times \delta \mathbf{E}_\perp^*) \cdot (\nabla \delta E_z \times \hat{\mathbf{e}}) dV \\ & \quad + \int_{\text{atm.}} \left(\frac{\omega}{c} \right)^2 \delta \mathbf{E}_\perp^* \cdot \delta \mathbf{E} dV. \end{aligned} \quad (6)$$

In deriving eq. (6) we use $\Delta \delta \mathbf{E} = -(\omega/c)^2 \delta \mathbf{E}$ in the atmosphere. Since we assume that c is infinite, the third term in r.h.s. of eq. (6) disappears. The first term is similar to the potential energy term in the magnetosphere. Then we write δE_z in the second term of eq. (6) in terms of $\delta \mathbf{E}_\perp$ by using $\nabla \delta \mathbf{E} = 0$ and $\delta B_y = 0$ (no toroidal magnetic perturbation) in the atmosphere. Combining eqs. (4), (5) and (6) we obtain the functional for the FEM calculations of the coupled MHD oscillations:

$$\begin{aligned} 0 &= \int_{\text{mag.}} (\nabla \times \delta \mathbf{E}_\perp^*) \cdot (\nabla \times \delta \mathbf{E}_\perp) dV + \int_{\text{atm.}} (\nabla \times \delta \mathbf{E}_\perp^*) \cdot (\nabla \times \delta \mathbf{E}_\perp) dV \\ & \quad - \int_{\text{atm.}} \frac{\partial \delta E_x^*}{\partial z} \cdot \frac{\partial \delta E_x}{\partial z} dV - \int_{\text{mag.}} \left(\frac{\omega}{V_A} \right)^2 \delta \mathbf{E}_\perp^* \cdot \delta \mathbf{E}_\perp dV \\ & \quad - i\omega \mu_0 \Sigma_P \int_{\text{ionos.}} \delta \mathbf{E}_\perp^* \cdot \delta \mathbf{E}_\perp dS - i\omega \mu_0 \Sigma_H \int_{\text{ionos.}} (\delta \mathbf{E}_\perp^* \times \delta \mathbf{E}_\perp) \cdot (-\hat{\mathbf{e}}) dS. \end{aligned} \quad (7)$$

The finite element discretization is done in x and z directions. As for element functions of $\delta \mathbf{E}_\perp$, the previous works (KRAUSS-VARBAN and PATEL, 1988; FUJITA and PATEL, 1992) employed the product of linear functions of x and z (or radial and field-aligned direction in a dipole field model) for δE_y (or azimuthal component) and product of the linear function of z and the constant function of x for δE_x (or radial component). In the present case we employ the same element functions. Discretization of $\delta \mathbf{E}_x$ is,

$$\delta E_x(x, z) = \sum_{i,j} \{X_{i+1/2,j} c_{i+1/2}(x) e_j(z)\}. \quad (8)$$

As for δE_y

$$\delta E_y(x, z) = \sum_{i,j} \{Y_{i,j} e_i(x) e_j(z)\}. \quad (9)$$

$X_{i+1/2,j}$ and $Y_{i,j}$ are nodal values for δE_x and δE_y .

2.4. Contribution from the neutral atmosphere

When we construct the FEM matrix equation from eq. (7) using the element functions and eqs. (8) and (9), it becomes

$$Ax + i\omega Cx + \omega^2 Bx = 0, \quad (10)$$

where A , C , and B are matrices and x is the FEM discretized nodal vector. The first and third terms of eq. (10) are derived from the potential energy and the kinetic energy parts. The second term indicates the ionospheric Joule dissipation due to the Pedersen current and the mode conversion due to the Hall current. When we divide x as

$$x = \begin{pmatrix} x_1 \\ x_2 \end{pmatrix}, \quad (11)$$

where x_1 and x_2 are the nodal vectors for the magnetosphere (including the ionosphere) and the atmosphere. Then matrix A can be divided as follows:

$$A = \begin{pmatrix} A_{11} & A_{12} \\ A_{21} & A_{22} \end{pmatrix}. \quad (12)$$

The element small matrix A_{11} is the contribution from the magnetosphere and the ionosphere. The element small matrix A_{22} comes from the atmosphere. On the other hand

$$B = \begin{pmatrix} B_{11} & 0 \\ 0 & 0 \end{pmatrix}, \quad (13)$$

because c is assumed infinite in the atmosphere. In addition

$$C = \begin{pmatrix} C_{11} & 0 \\ 0 & 0 \end{pmatrix}. \quad (14)$$

From eqs. (10) to (14) we obtain

$$A_{11}x_1 + A_{12}x_2 + i\omega C_{11}x_1 + \omega^2 B_{11}x_1 = 0, \quad (15)$$

and

$$A_{21}x_1 + A_{22}x_2 = 0. \quad (16)$$

From eq. (16), it follows that

$$x_2 = -A_{22}^{-1}A_{21}x_1. \quad (17)$$

Finally eq. (15) becomes

$$(A_{11} - A_{12}A_{22}^{-1}A_{21})\mathbf{x}_1 + i\omega C_{11}\mathbf{x}_1 + \omega^2 B_{11}\mathbf{x}_1 = 0. \quad (18)$$

We can evaluate the contribution from the atmosphere using eq. (18).

3. Numerical Results

When $m=0$ the usual coupled oscillation theory excluding the ionospheric effect indicates no resonant MHD oscillations. But if the anisotropic conducting ionosphere modifies the MHD oscillations, what will happen? Here we present numerical results. The ionospheric conductivities are normalized to $\mu_0 V_0$ where $V_0 = V_A$ at $(x, z) = (1, 0)$, the equator on the outer boundary. The thickness of the atmosphere (d) is 0.01. The oscillation frequency ω is normalized to l_{\parallel}/V_0 where l_{\parallel} is the field-aligned distance between the ionosphere and the equator ($l_{\parallel} = 1$ for the present model). The intensity of electric perturbation is normalized to its maximum intensity. Numerals shown in the upper left corner of each figure indicates the maximum intensity. Note that δE_x and δE_y have phase difference of $\pi/2$. Since the present numerical calculation is based on a linear MHD theory, the intensity itself does not make sense. Only the relative intensity $\delta E_x/\delta E_y$ is physically important.

Figure 2a shows the spatial structure of electric field perturbations in the northern hemisphere when $\Sigma_p=0$, $\Sigma_H=1$, and $m=0$. The electric perturbations are symmetric with respect to the equator because this mode is the fundamental global mode oscillation.

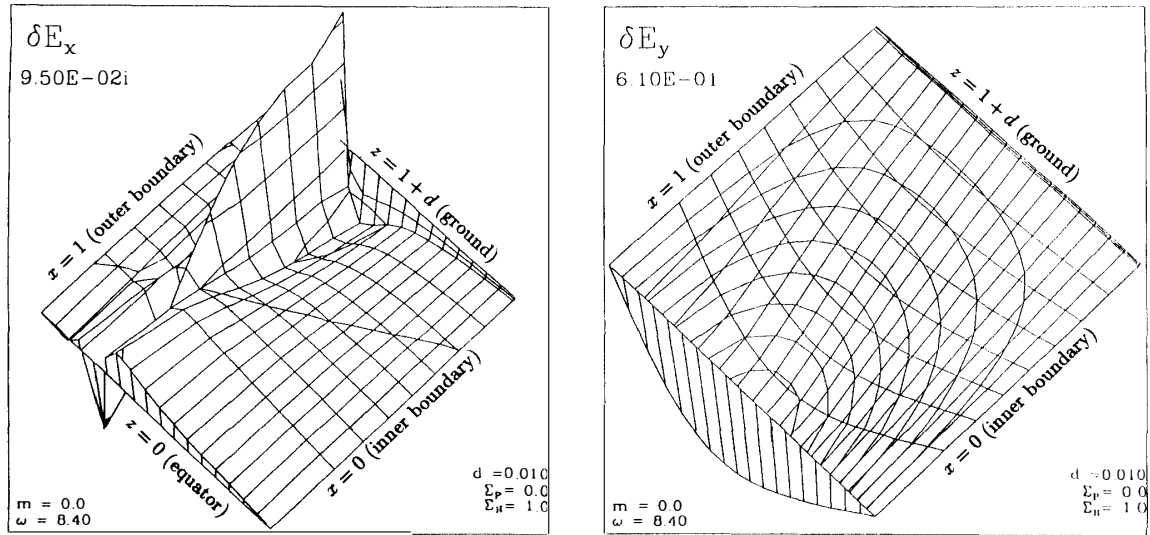


Fig. 2a.

Fig. 2. Spatial structures of the electric field perturbations associated with the fundamental global mode oscillation in the northern hemisphere when $m=0$ and $d=0.01$. (a) $\Sigma_p=0$ and $\Sigma_H=1$ ($\omega=8.40$), (b) $\Sigma_p=1$ and $\Sigma_H=1$ ($\omega=8.40 - 2.60 \times 10^{-4}i$), (c) $\Sigma_p=10$ and $\Sigma_H=1$ ($\omega=8.40 - 1.16 \times 10^{-3}i$). Note that δE_x and δE_y have phase difference of $\pi/2$. The numeral in the upper left corner of each figure indicates the maximum electric field intensity obtained directly from the calculation. The coordinate (x, z) of the bottom mesh point in each figure is $(1, 0)$ and that of the uppermost point is $(0, 1+d)$. The ionosphere lies on the line $z=1$.

tion. It is evident that δE_x is enhanced on certain field lines from this figure. This field line is referred to as the resonant field line. Figure 2a shows that the field-aligned structure of δE_x is apt to be maximum on the ionosphere. This means that the electric perturbation of the Alfvén wave (δE_x) has the antinode on the ionosphere. We also point out that δE_y does not show resonant behavior on that field line. One may suppose that coarse grids do not reproduce enhancement in δE_y if the enhancement is confined to the area much smaller than the distance between two grids. To answer this question, we locate the mesh grid where δE_x is enhanced (the resonant field line) on slightly different places. As a result we do not observe any enhancement in δE_y . Therefore we conclude that δE_y is not enhanced on the resonant field line.

We should mention here that there is no δE_x when Σ_H is zero. We only have the spatial distribution of δE_y , like that in Fig. 2a. Since δE_x (the Alfvén-mode electric field)

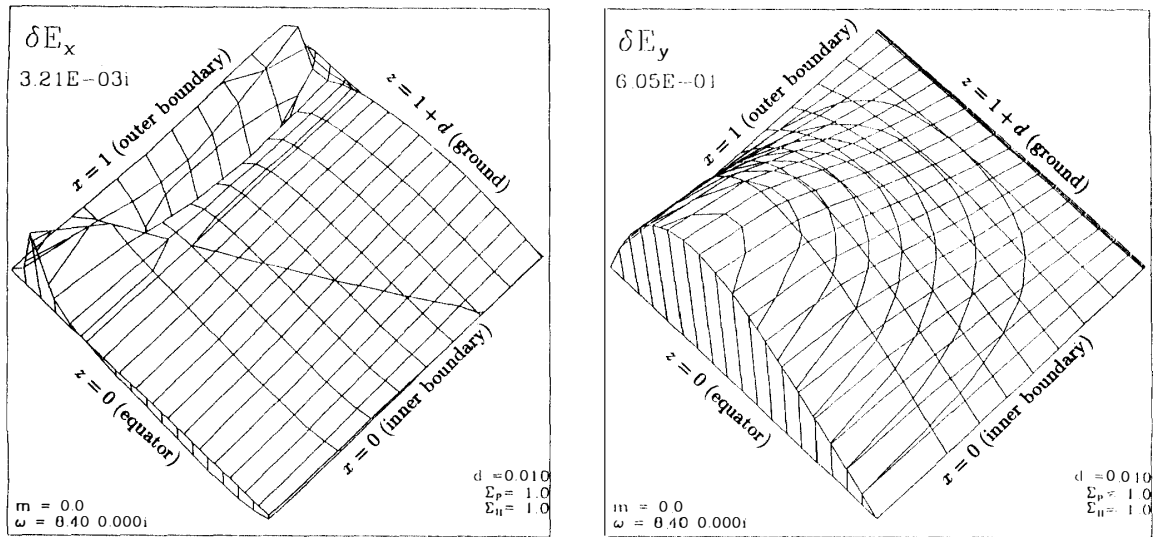


Fig. 2b.

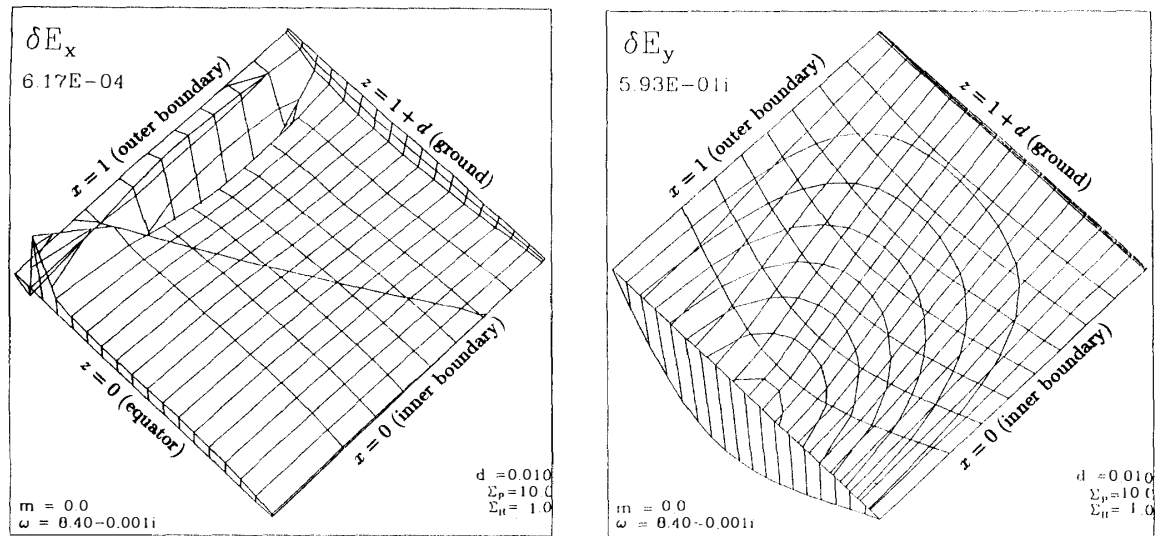


Fig. 2c.

is generated through the ionospheric Hall current, this result is natural.

Next we present Figs. 2b and 2c which show the structures of the electric field perturbations when Σ_p is nonzero ($\Sigma_p=1$ and 10 for Figs. 2b and 2c). The values of Σ_H and d are the same as those for Fig. 2a. In this case we have again an enhanced δE_x . But δE_x does not have an antinode on the ionosphere. After examining carefully the numerical results, we find that the location of the resonant field line is different from that for the case of $\Sigma_p=0$. This is attributed to the fact that the larger Σ_p imposes δE tangential to the ionosphere to have a node on the ionosphere. The structure of δE_y is the same as that in the case of $\Sigma_p=0$. When comparing the amplitude of the Alfvén wave (δE_x) relative to that of the fast mode wave (δE_y), the ratio becomes smaller as Σ_p becomes greater. This feature indicates that the mode conversion due to the ionospheric Hall current is less effective when Σ_p becomes greater. The reason is ascribed to the reduced intensity of the electric perturbation on the ionosphere for larger Σ_p . Extremely large Σ_p yields perfect reflection of the wave *i.e.* no electric field on the ionosphere.

The eigenfrequency is naturally a complex number when Σ_p is nonzero. The negative imaginary part shows the damping of the oscillation due to the ionospheric Joule dissipation.

We should mention here that the present calculation employs coarse mesh grids due to limited capacity of the computer of the Meteorological Research Institute. Thus we don't show another calculation for nonzero m . As long as we consider behavior of coupled oscillations due to the ionospheric Hall current, the present calculation sufficiently reproduces a real feature of the coupled oscillations.

4. Discussion and Concluding Remarks

4.1. Validity of the present numerical results

Owing to limited capacity of the computer we cannot help but use coarse mesh grids for the present numerical calculations. Therefore we need to consider the validity of the results.

We pointed out from the present numerical calculations the following features of the coupled oscillation affected by the ionospheric Hall current:

- (1) There is an enhancement in δE_x when Σ_H is nonzero. δE_x is not generated when Σ_H is zero.
- (2) δE_x has a node/an antinode on the ionosphere when Σ_p is smaller/larger.
- (3) The eigenfrequency becomes a complex number when Σ_p is nonzero. When Σ_p becomes larger, the imaginary part grows larger.
- (4) δE_x is enhanced along the resonant field line but δE_y is not.

The features (1) and (2) are obvious in Fig. 2 even though the mesh grids are coarse. Enhancement in δE_x (the Alfvén-mode electric field) is analogous to an externally forced oscillation in the case that the frequency of the external wave matches that of an oscillator. In the present case the external force is the oscillatory ionospheric Hall current induced by the electric field of the fast mode wave. This current produces the resonant Alfvén wave in the magnetosphere. The second feature can be understood because the ionospheric Pedersen current partly reflects an oscillatory em field. Taking into account that the ionospheric Pedersen current dissipates em energy of the oscilla-

tion, we can understand feature (3). But due to an insufficient number of mesh grids we cannot believe all digits of ω_i are accurate. We only insist on the tendency that larger Σ_p yields larger ω_i . But too large Σ_p will again reduce ω_i although we do not show the relevant numerical result here. The reason is that the ionosphere with extremely large Σ_p reflects perfectly em fields of MHD waves. The last feature needs further verification. To exclude possibility that the area of enhanced δE_y falls into the gap between two mesh grids, we move slightly one mesh grid on which δE_x is enhanced. As a result we conclude that there is no enhancement in δE_y .

4.2. Behavior of δE_y

Let us consider analytically the behavior of the MHD oscillations affected by the ionospheric currents. The magnetospheric Alfvén speed V_A is assumed to be uniform in the z direction in the following discussion.

As we stress on the mode coupling due to the Hall current, m is assumed to be zero. Then the equations of the MHD oscillations are

$$\frac{\partial^2 \delta E_x}{\partial z^2} = \left(\frac{\omega}{V_A} \right)^2 \delta E_x, \quad (19)$$

for the Alfvén wave and

$$\left(\frac{\partial^2}{\partial x^2} + \frac{\partial^2}{\partial z^2} \right) \delta E_y = \left(\frac{\omega}{V_A} \right)^2 \delta E_y, \quad (20)$$

for the fast mode wave. For the correspondence to the numerical calculations δE_x and δE_y are assumed to have antinodes at $z=0$ (the equator). When the model is uniform along the z direction, the solutions of eqs. (19) and (20) are

$$\delta E_x(z, x) = \delta E_{x0}(x) \cos \{K(x)z\}, \quad (21)$$

where $K(x) = \omega/V_A(x)$ and

$$\delta E_y(z, x) = \delta E_{y0}(x) \cos(kz). \quad (22)$$

The functions, $\delta E_{x0}(x)$ and $\delta E_{y0}(x)$, which are electric field amplitudes of δE_x and δE_y on the ionosphere, are determined by boundary conditions. On the ionosphere ($z = \pm 1$) the ionosphere current yields a discontinuity in magnetic field perturbations (eqs. (3) and (4)). The condition of no toroidal magnetic field perturbation in the atmosphere results in the following equation:

$$\mu_0 \Sigma_H \delta E_{y0}(x) \cos k = \left[\frac{K(x) \sin \{K(x)\}}{i\omega} + \mu_0 \Sigma_P \cos \{K(x)\} \right] \delta E_{x0}(x). \quad (23)$$

Using eqs. (20) and (23), we obtain

$$\begin{aligned} \frac{d^2}{dx^2} \left(\left[\frac{K(x) \sin \{K(x)\}}{i\omega} + \mu_0 \Sigma_P \cos \{K(x)\} \right] \delta E_{x0}(x) \right) \\ = \{k^2 - K(x)^2\} \left[\frac{K(x) \sin \{K(x)\}}{i\omega} + \mu_0 \Sigma_P \cos \{K(x)\} \right] \delta E_{x0}(x). \end{aligned} \quad (24)$$

We consider only the case where $\Sigma_p = 0$. Since there is no energy dissipation, the

frequency of the MHD oscillation becomes a real number. Consequently the coefficient of $d^2\delta E_{x0}(x)/dx^2$ becomes zero at x_0 of $\sin\{K(x_0)\}=0$. Setting $\Sigma_p=0$ and expanding eq. (24) around $x=x_0$, we obtain a confluent type differential equation with the pole at $x=x_0$. The behavior of the solution near $x=x_0$ is

$$\delta E_{x0}(x) \propto \frac{1}{x-x_0}. \quad (25)$$

Consequently δE_x becomes singular at $x=x_0$. Namely the Alfvén wave is resonant with the fast mode wave at a resonant field line of $\sin\{K(x)\}=0$. Applying eq. (25) to eq. (23) with $\Sigma_p=0$ we find that $\delta E_{y0}(x) \propto K_0 \dot{K}_0$. This means that the electric perturbation of the fast mode does not have singularity at $x=x_0$. The electric perturbation of the Alfvén wave is singular along a resonant field line, but that of the fast mode is not enhanced.

As noted previously, we checked through a numerical way that the behavior of em fields along the resonant field line does not change when the location of the resonant field line shifts. We must confess that the above discussion is not complete because the poloidal magnetic component is disregarded. However, the problem becomes eventually an eigenvalue problem solved in the present paper if both toroidal and poloidal components are considered. It is impossible to treat it in an analytical way.

4.3. Characteristics of resonance coupling due to the ionospheric Hall current

Note that δE_x and δE_y are assumed to be antisymmetric with respect to the equator (eqs. (21) and (22)). When they are symmetric, the result is the same as stated above. But when one component is symmetric and the other is antisymmetric, there is no resonance because the ionospheric boundary condition (eq. (23)) in one hemisphere becomes different from that in the other hemisphere.

Now we compare the resonance due to the Hall current with that due to the nonuniformity of field. As shown by CHEN and COWLEY (1989) and FUJITA and PATEL (1992), the electric field perturbations of Alfvén wave and of fast mode wave behave singularly on a resonant field line for the coupled MHD oscillations in the inhomogeneous fields. Unlike this only the Alfvén-mode electric perturbation is enhanced in the present case. The resonance condition for the coupled MHD oscillations in the nonuniform field is $K(x)=k$ (SOUTHWOOD, 1974). Namely δE_x and δE_y of the oscillation have the same field-aligned structure on a resonant field line. On the other hand, the resonance condition for the present case is $\sin\{K(x)\}=0$ for the antisymmetric mode or $\cos\{K(x)\}=0$ for the symmetric mode. In other words, the resonance coupling occurs, for example, even when the Alfvén wave has the third harmonic mode structure (three antinodes) along the ambient field line and the fast mode wave has the fundamental mode structure (one antinode). Therefore unlike the coupled MHD oscillations in the inhomogeneous field the field-aligned structure of δE_x generally differs from that of δE_y on the resonant field line.

When Σ_p is nonzero, the Joule dissipation at the ionosphere results in a complex frequency of the MHD oscillation. Consequently there is no singularity of eq. (24). But we expect the enhanced electric field perturbation of the Alfvén wave on the field line whose eigenfrequency matches the eigenfrequency of the global fast mode oscillation.

Comparing with the case of $\Sigma_p = 0$ where the amplitude of δE_x becomes quite large, δE_x is slightly enhanced when Σ_p is nonzero due to the dissipation. The enhancement is similar to the damped oscillation forced by the external oscillation with the resonance frequency.

4.4. Other remarks

We discuss a possibility of the field line resonance due to the ionospheric Hall current. The actual ionosphere usually has Σ_H larger than Σ_p . Thus this condition is favorable to enhanced Alfvén-mode field perturbations due to the coupling. Furthermore suppose that the solar wind push the dayside magnetosphere, various waves with various azimuthal wave numbers are generated in the magnetosphere. We can expect that there is a component with the azimuthally uniform wave field. Therefore the resonance coupling through the ionospheric Hall current takes place in the magnetosphere. The coupled oscillations thus generated are characterized with the enhanced Alfvén-mode component and smaller fast-mode component. The data analysis done by TAKAHASHI *et al.* (1988) which reported the existence of the enhanced Alfvén mode oscillation without any fast-mode oscillation at the same frequency may be explained by the present theory.

It is possible to investigate further physical characteristics of the coupled MHD oscillations by showing structures of the magnetic field perturbations, electric currents and Poynting flux (energy flow). We plan to present such results in an other full paper.

4.5. Summary

We present in this paper the formulation of the FEM calculations of the coupled MHD oscillations in the magnetosphere-ionosphere system. By using the simple box model with the anisotropically conducting thin ionosphere and the insulating atmosphere, we obtain important results on the coupled oscillation associated with the ionospheric Hall current:

1) When m (corresponding to the azimuthal wave number for the actual magnetosphere) is zero, there is the resonance coupling of the MHD oscillations due to the ionospheric Hall current if $\Sigma_p = 0$. The electric field perturbation of the Alfvén wave is maximized in the ionosphere.

2) When Σ_p is nonzero and $m = 0$, the enhanced Alfvén wave is still generated. Unlike the case of $\Sigma_p = 0$, the electric field perturbations do not have the maximum intensity in the ionosphere.

3) The fast-mode perturbation is not enhanced in the case of Hall-current-generated resonance.

Acknowledgments

The author is very grateful to Dr. V. L. PATEL of Plasma Physics Division, Naval Research Laboratory for introducing him to this field of research. He is thankful to Dr. M. ITONAGA of Kyushu University for useful discussion on formulation of em field perturbations in the atmosphere. He is also indebted to Prof. M. SUGIURA of Tokai University, Prof. Y. INOUE of Kyoto Sangyo University and Dr. A. MIURA of

University of Tokyo for their kind help of collecting reference papers. Numerical calculations were performed by the computers of Meteorological Research Institute and of National Institute of Polar Research.

References

- ALLAN, P., WHITE, S. P. and POULTER, E. M. (1986a): Impulsive-excited hydromagnetic cavity and field-line resonances in the magnetosphere. *Planet. Space Sci.*, **34**, 371–385.
- ALLAN, P., POULTER, E. M. and WHITE, S. P. (1986b): Hydromagnetic wave coupling in the magnetosphere —Plasmapause effects on impulse-excited resonances. *Planet. Space Sci.*, **34**, 1189–1200.
- CHEN, L. and COWLEY, S. C. (1989): On the field line resonance of hydromagnetic Alfvén waves in dipole magnetic field. *Geophys. Res. Lett.*, **16**, 895–897.
- FUJITA, S. (1988): Duct propagation of hydromagnetic waves in the upper ionosphere, 2, Dispersion characteristics and loss mechanism. *J. Geophys. Res.*, **93**, 14674–14682.
- FUJITA, S. and PATEL, V. L. (1992): Eigenmode analysis of coupled magnetohydrodynamic oscillations in the magnetosphere. *J. Geophys. Res.*, **97**, 13777–13788.
- FUJITA, S. and TAMAO, T. (1988): Duct propagation of hydromagnetic waves in the upper ionosphere, 1, Electromagnetic field disturbances in high latitudes associated with localized incidence of a shear Alfvén wave. *J. Geophys. Res.*, **93**, 14665–14673.
- GRUBER, R. and RAPPAZ, J. (1985): *Finite Element Methods in Linear Ideal Magnetohydrodynamics*. New York, Springer.
- HAMEIRI, E. and KIVELSON, M. G. (1991): Magnetospheric waves and the atmosphere-ionosphere layer. *J. Geophys. Res.*, **96**, 21125–21134.
- HUGHES, W. J. and SOUTHWOOD, D. J. (1976a): The screening of micropulsation signals by the atmosphere and ionosphere. *J. Geophys. Res.*, **81**, 3234–3240.
- HUGHES, W. J. and SOUTHWOOD, D. J. (1976b): An illustration of modification of geomagnetic pulsation structure by the ionosphere. *J. Geophys. Res.*, **81**, 3241–3247.
- INOUE, Y. (1973): Wave polarizations of geomagnetic pulsations observed in high latitudes on the Earth's surface. *J. Geophys. Res.*, **78**, 2959–2976.
- INOUE, Y. and HOROWITZ, S. (1966a): Magneto-ionic coupling in an inhomogeneous anisotropic medium. *Radio Sci.*, **1**, 427–440.
- INOUE, Y. and HOROWITZ, S. (1966b): Numerical solution of full-wave equation with mode coupling. *Radio Sci.*, **1**, 957–970.
- INOUE, Y. and SHAEFFER, D. L. (1970): Full wave solution for the transmission of ULF and ELF waves through the ionosphere. Air Force Cambridge Res. Labs., AFCRL Report No. 70-0531.
- KIVELSON, M. G. and SOUTHWOOD, D. J. (1985): Resonant ULF waves: A new interpretation. *Geophys. Res. Lett.*, **12**, 49–52.
- KIVELSON, M. G. and SOUTHWOOD, D. J. (1988): Hydromagnetic waves and the ionosphere. *Geophys. Res. Lett.*, **15**, 1271–1274.
- KRAUSS-VARBAN, D. and PATEL, V. L. (1988): Numerical analysis of the coupled hydromagnetic wave equations in the magnetosphere. *J. Geophys. Res.*, **93**, 9721–9729.
- LEE, D.-H. and LYSAK, R. (1989): Magnetospheric ULF wave coupling in the dipole model: The impulsive excitation. *J. Geophys. Res.*, **94**, 17097–17103.
- LEE, D.-H. and LYSAK, R. (1990): Effects of azimuthal asymmetry on ULF waves in the dipole magnetosphere. *Geophys. Res. Lett.*, **17**, 53–56.
- LEE, D.-H. and LYSAK, R. (1991a): Impulsive excitation of ULF waves in the three-dimensional dipole model: The initial results. *J. Geophys. Res.*, **96**, 3479–3486.
- LEE, D.-H. and LYSAK, R. (1991b): Monochromatic ULF wave excitation in the dipole magnetosphere. *J. Geophys. Res.*, **96**, 5811–5817.
- SOUTHWOOD, D. J. (1974): Some features of field-line resonances in the magnetosphere. *Planet. Space Sci.*, **22**, 483–491.
- TAKAHASHI, K., KISTLER, L. M., POTEMRA, T. A., MCENTIRE, R. W. and ZANETTI, L. J. (1988):

Magnetospheric ULF waves observed during the major magnetospheric compression of November 1, 1984. *J. Geophys. Res.*, **93**, 14369–14382.

ZIENKIEWICS, O. C. and TAYLOR, R. L. (1989): *The Finite Element Method*, 4th ed. London, McGraw-Hill.

(Received March 20, 1992; Revised manuscript received September 17, 1992)